Am. J. Hum. Genet. 65:645–655, 1999

The Phenotypic Spectrum of GLI3 Morphopathies Includes Autosomal Dominant Preaxial Polydactyly Type-IV and Postaxial Polydactyly Type-A/B; No Phenotype Prediction from the Position of GLI3 Mutations

Uppala Radhakrishna,[1] Dorothea Bornholdt,[2] Hamish S. Scott,[1] Uday C. Patel,[3] Colette Rossier,[1] Hartmut Engel,[2] Armand Bottani,[4] Divya Chandal,[5] Jean-Louis Blouin,[4] Jitendra V. Solanki,[3] Karl-Heinz Grzeschik,[2] and Stylianos E. Antonarakis[1,4,6]

[1]Division of Medical Genetics, University of Geneva Medical School and [4]University Hospital, Geneva; [2]Institute of Human Genetics, Philipps University, Marburg, Germany; [3]Department of Animal Genetics and Breeding, Veterinary College, Gujarat Agriculture University, Anand, and [5]Department of Zoology, Gujarat University, Ahmedabad, India

Summary

Functional characterization of a gene often requires the discovery of the full spectrum of its associated phenotypes. Mutations in the human GLI3 gene have been identified in Greig cepalopolysyndactyly, Pallister-Hall syndrome (PHS), and postaxial polydactyly type-A (PAP-A). We studied the involvement of GLI3 in additional phenotypes of digital abnormalities in one family (UR003) with preaxial polydactyly type-IV (PPD-IV), three families (UR014, UR015, and UR016) with dominant PAP-A/B (with PPD-A and -B in the same family), and one family with PHS. Linkage analysis showed no recombination with GLI3-linked polymorphisms. Family UR003 had a 1-nt frameshift insertion, resulting in a truncated protein of 1,245 amino acids. A frameshift mutation due to a 1-nt deletion was found in family UR014, resulting in a truncated protein of 1,280 amino acids. Family UR015 had a nonsense mutation, R643X, and family UR016 had a missense mutation, G727R, in a highly conserved amino acid of domain 3. The patient with PHS had a nonsense mutation, E1147X. These results add two phenotypes to the phenotypic spectrum caused by GLI3 mutations: the combined PAP-A/B and PPD-IV. These mutations do not support the suggested association between the mutations in GLI3 and the resulting phenotypes. We propose that all phenotypes associated with GLI3 mutations be called "GLI3 morphopathies," since the phenotypic borders of the resulting syndromes are not well defined and there is no apparent genotype-phenotype correlation.

Received April 30, 1999; accepted for publication July 9, 1999; electronically published August 10, 1999.

Address for correspondence and reprints: Dr. Stylianos E. Antonarakis, Division de Génétique Médicale, Centre Médical Universitaire, 1 rue Michel-Servet, 1211 Geneva 4, Switzerland. E-mail: Stylianos.Antonarakis@medecine.unige.ch

0002-9297/1999/6503-0009$02.00

Introduction

The study of natural mutations resulting in clinically recognized human dysmorphic syndromes has recently made important contributions to our knowledge of the potential function of genes in human development (Epstein 1995). In the past 5 years, molecular dysmorphology has begun to provide diagnostic tests for the exact characterization of developmental anomalies.

Mutations in the human transcription regulator gene GLI3 (fig. 1) are associated with three autosomal dominant phenotypes: the Greig cephalopolysyndactyly syndrome (GCPS; MIM175700) (Vortkamp et al. 1991; Wild et al. 1997), Pallister-Hall syndrome (PHS; MIM 146510) (Kang et al. 1997*a*), and postaxial polydactyly type A (PAP-A; MIM 147200) (Radhakrishna et al. 1997*b*). Most of the clinical characteristics of these syndromes are distinct, but all share digital abnormalities. It has been suggested that there is an association between the site of GLI3 protein truncation and the phenotypes in syndromes caused by GLI3 mutations (Biesecker 1997): GCPS is caused by protein truncations before or within the zinc finger domain (ZFD) (Wild et al. 1997), PHS by truncations after the ZFD but before the Post zinc finger domain 1 (Pzf1, or domain 3) (Ruppert et al. 1990), whereas PAP-A is associated with mutations after domain 3 (Radhakrishna et al. 1997*b*).

The human GLI3 is homologous to the Drosophila Cubitus interruptus (*Ci*) (Orenic et al. 1990). *Ci* is a transcription regulator and an important component of the hedgehog signaling pathway of pattern formation of limbs and wings (Dominguez et al. 1996). Full-length *Ci* (Ci^{155}) is localized in the cytoplasm, where it is anchored to the microtubule system. In the absence of hedgehog, *Ci* is cleaved by a hedgehog-regulated protease to generate an amino-terminal fragment (Ci^{75}) containing the ZFD, which is subsequently translocated to the nucleus where it represses its target genes (Aza-Blanc et al. 1997; Robbins et al. 1997; Ruiz i Altaba 1997;

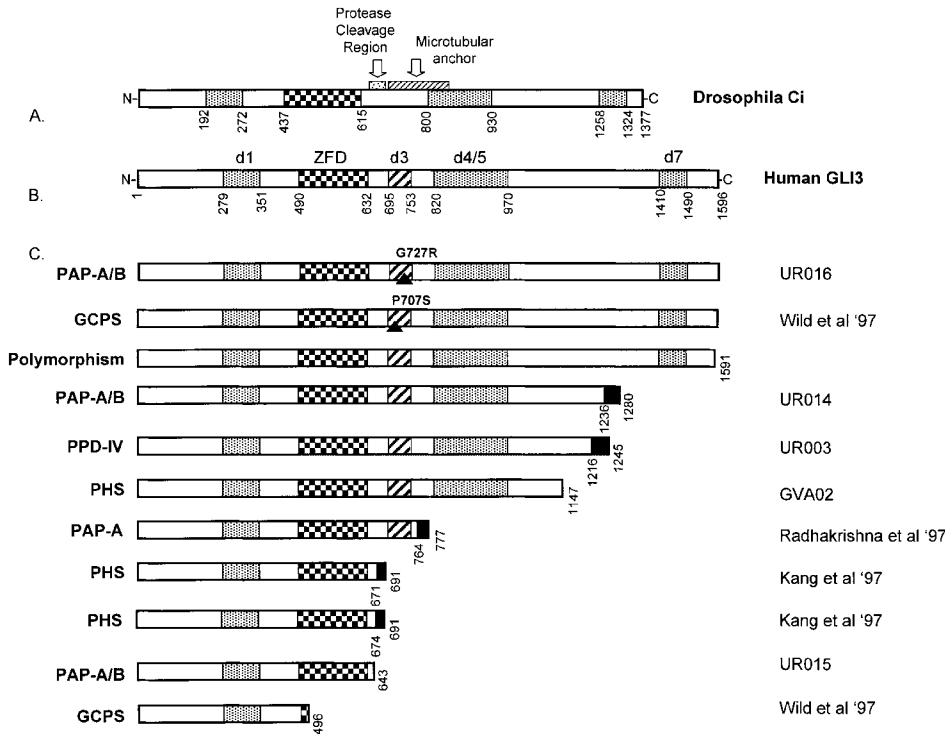

Figure 1 *A,* Schematic representation of Drosophila *Ci* protein and its identified domains, protein cleavage region, and microtubular anchor sequences. *B,* GLI3 protein showing the homologous domains with *Ci. C,* Schematic representation of the predicted GLI3 proteins in five different (GCPS, PHS, PAP-A, PAP-A/B, PPD-IV) autosomal dominant traits. The blackened domain at the carboxyl-terminus of some predicted mutant proteins depicts the novel abnormal amino acids. The families described here corresponding to the mutant proteins or to the literature citation are depicted to the right of the schematic of each mutant protein.

Sisson et al. 1997). In contrast, in the presence of hedgehog signaling, Ci^{155} translocates to the nucleus and activates transcription. It is not clear whether the human GLI3 protein undergoes similar proteolytic cleavage, cellular trafficking, and regulation of transcriptional activity as the Drosophila *Ci.* However, if this is the case, then the processing of the predicted truncated GLI3s found in the various syndromes may be altered and directly implicated with different GLI3 phenotypes. It has been shown, by means of truncated GLI3 proteins in transfection experiments in mammalian cells, that selected GLI3 truncations mimic the Drosophila *Ci* protein functions and subcellular localization (Shin et al. 1999). They showed that full-length GLI3 (which is similar to Ci^{155}) localizes to the cytoplasm and activates Patched 1 (PTCH1) expression; a mutant truncated GLI3 of the first 674 amino acids (which is similar to Ci^{75}) localizes to the nucleus and represses GLI3-activated PTCH1 expression (Shin et al. 1999).

The associations of different dysmorphic phenotypes with different GLI3 mutations are made on the basis of only a few cases; in addition, an amino acid substitution, P707S, within domain 3, has been found in a patient with GCPS (Wild et al. 1997).

To further elucidate the involvement of GLI3 mutations in polydactyly syndromes, and to contribute to the attractive hypothesis of genotype-phenotype correlation on the basis of sites of the mutations, we have investigated the molecular basis of patients with PAP-A/B, with preaxial polydactyly type-IV (PPD-IV; MIM 174700) and with PHS.

Families with PAP-A/B include individuals with both type A (PAP-A) and type B (PAP-B) (Kucheria et al. 1981). In PAP-A, the extra digit is well formed, articulates with the 5th or extra metacarpal/metatarsal, and is usually functional. In PAP-B (pedunculated postminimus), the extra digit is not well formed and frequently occurs in the form of a skin tag (Temtamy and McKusick 1969). The PPD-IV family was studied because of the clinical suggestion that this abnormality may be allelic to GCPS (Baraitser et al. 1983).

We report that, at least in certain families, PAP-A/B and PPD-IV are also due to mutations in GLI3. The location of the mutation and the structure of the predicted abnormal protein do not conform to the hypothesis suggested by Biesecker (1997); and the genotype-phenotype correlation, if it exists at all for phenotypes caused by GLI3 mutations, is not obvious. In addition,

we propose the term "GLI3 morphopathies" to describe the spectrum of phenotypes related to mutations in GLI3 (presently including GCPS, PHS, PAP-A, PAP-A/B, and PPD-IV), and that these various clinical syndromes represent a continuum of phenotypes with unclear limitations.

Subjects, Material, and Methods

Family UR003

Family UR003 is from the Gujarat state in western India and has PPD-IV. The pedigree consists of 35 individuals including 22 who are affected (partial pedigree is shown in fig. 2*A*, and hand/foot phenotypes are shown in fig. 2*D–I*). Most affected individuals had bilateral anomalies in their lower limbs although their hands were less-severely affected, and some individuals had apparently normal hands. Foot polydactyly was the only abnormality in 12 of the 22 affected individuals. The anomaly ranges from duplication of the big toe(s) (double toes) to syndactyly of toes with PAP. Hand polydactyly was not observed without foot polydactyly. A few individuals showed only foot PAP, whereas 10 persons showed both hand and foot polydactyly. The more-severely affected individuals with hand polydactyly had bilateral duplication of the 5th fingers and nails and unilateral triplication of the 5th finger. One individual had duplication of 5th-finger nails in one hand and PAP-B in the other. Most hand abnormalities were combinations of unilateral or bilateral PAP-A or -B. In several affected individuals, the last toe (postaxially) was disproportionately larger than the previous one. Soft-tissue syndactyly of 2d and 3d toes was observed in three individuals. There is, therefore, extensive variability of the phenotypic features of a single molecular defect in this family. This trait was disadvantageous to a few of the affected individuals; however, no surgical corrections were performed. There were no craniofacial signs, such as frontal bossing, macrocephaly, hypertelorism, or broad base of the nose, in any of the individuals with the digital anomalies.

Family UR014

This three-generation pedigree, also from Gujarat, consists of a total of 18 individuals; 3 are affected males and 4 are affected females with dominant PAP-A/B (fig. 3*A*). Figure 3*D–I* shows clinical photographs and radiographs of phenotypic characteristics of selected individuals. All affected individuals examined showed extra digits in hands and feet. The extra digits were not well developed in the hands of all affected individuals. The phenotype was highly variable within the family, and it ranges from fully bilateral PAP-A in the hands with normal feet (one individual); PAP-A in the left hand and PAP-B in the right hand with normal feet (one individual); bilateral PAP-A in the hands and feet (three individuals); PAP-A in the right hand and bilateral PAP of the feet with soft-tissue syndactyly of the 5th and 6th toes in the right foot (one individual); to bilateral PAP-A of the hand with soft-tissue syndactyly of the 4th and 5th fingers and normal toes (one individual). X-rays of selected individuals with a PAP-A functional extra finger show that the additional fingers articulate with the 5th metacarpal. Some individuals showed broad thumbs.

Family UR015

This family also shows the phenotype of dominant PAP-A/B. Among 37 subjects in five generations of this pedigree from Gujarat (fig. 4*A*), there were 6 affected females and 10 affected males. In most affected individuals, polydactyly was observed in both hands and feet (fig. 4*D–G*). In this pedigree, one individual was found to have PAP-B in the right hand and PAP-A in the left hand with bilateral PAP of the feet. Most affected individuals could not use or move the 6th fingers. An associated anomaly observed in this family was soft-tissue syndactyly. Syndactyly of 2nd and 3rd toes in four individuals, unilateral syndactyly of 2nd and 3rd toes in six individuals, and syndactyly of 5th and 6th toes in four individuals were observed.

Family UR016

This four-generation pedigree, also from Gujarat, consists of 23 individuals, 8 of whom are affected with dominant PAP-A/B (fig. 5*A*). Clinical examination revealed the presence of both PAP-A and PAP-B, even within the same individual (fig. 5*D–G*). A bilateral boneless skin tag next to the 5th fingers (pedunculated postminimus) was observed in individuals with or without PAP of the feet. For example, one individual showed PAP-A in the left hand and PAP-B in the right hand and bilateral PAP in his lower limbs. An affected female showed PAP-A in her hands without any foot anomaly. The remaining affected individuals showed PAP-A of the upper and lower extremities.

Most affected individuals in the three families (UR014, UR015, and UR016) with PAP-A/B could not normally flex their additional fingers; hence, the extra fingers were not functional. In several individuals, the additional 6th digit was connected to the 5th finger with soft tissue only. No recognizable PAP-B polydactyly in the lower extremities was observed in any of the members of these families. All affected individuals with foot polydactyly had fully developed extra toes, and, in some instances, the additional 6th toe was larger than the 5th. The PAP trait was disadvantageous in most of the affected individuals; however, surgical corrections were performed in only a few of them. None of the affected

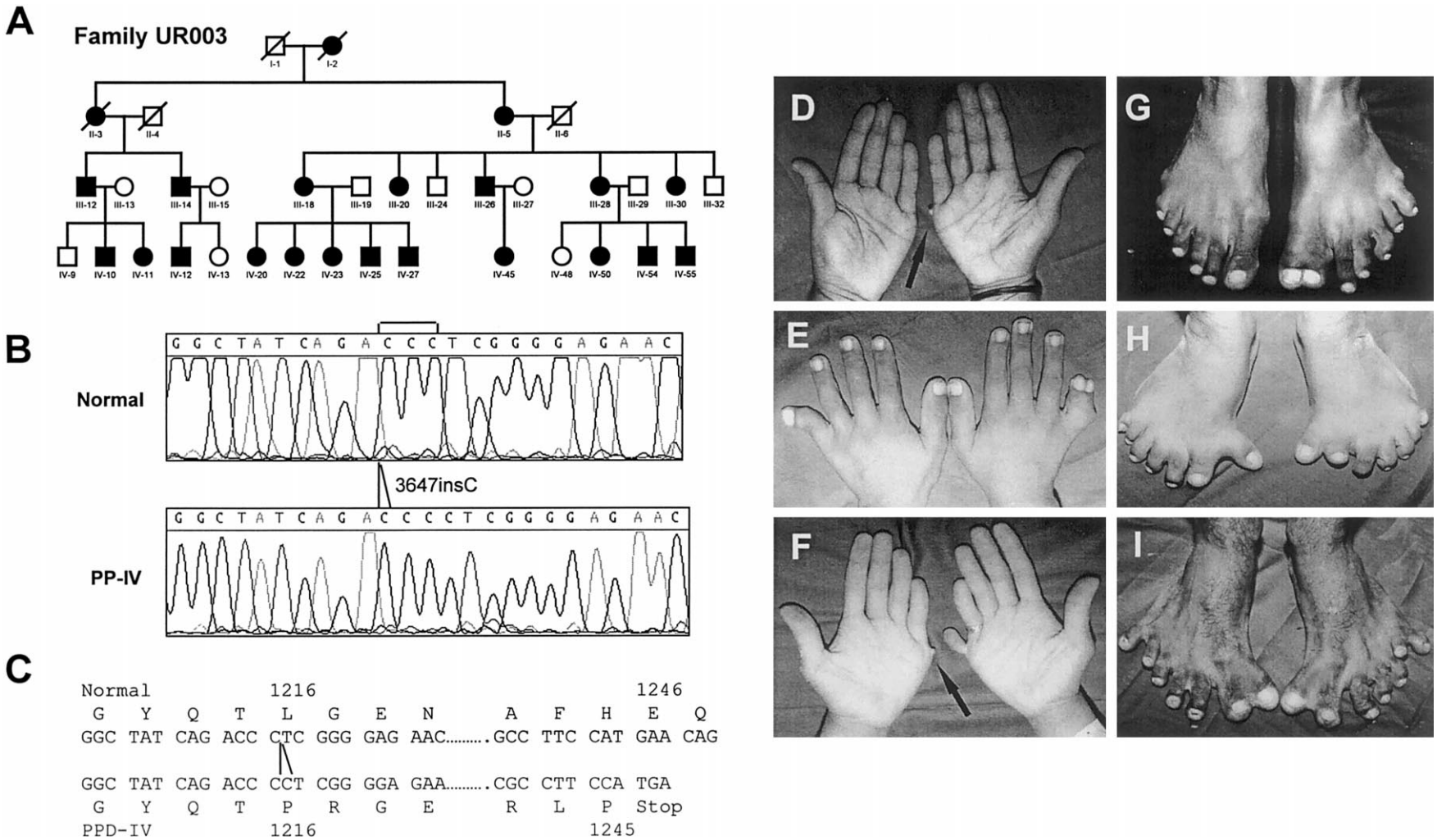

Figure 2 *A,* Partial pedigree of UR003 with PPD-IV. Affected individuals are shown with blackened symbols, and normal individuals are shown with unblackened symbols. *B,* Sequence comparison of a normal and mutant partial chromatograph of DNA from family UR003. The insertion of a C at nucleotide position 3647 of human GLI3 is shown. *C,* Comparison of translated products of normal and mutant human GLI3 alleles. The mutated protein is predicted to terminate at codon 1246 after the addition of 30 novel amino acids. *D–I,* Clinical photographs of six different affected individuals from family UR003, demonstrating the phenotypic variability.

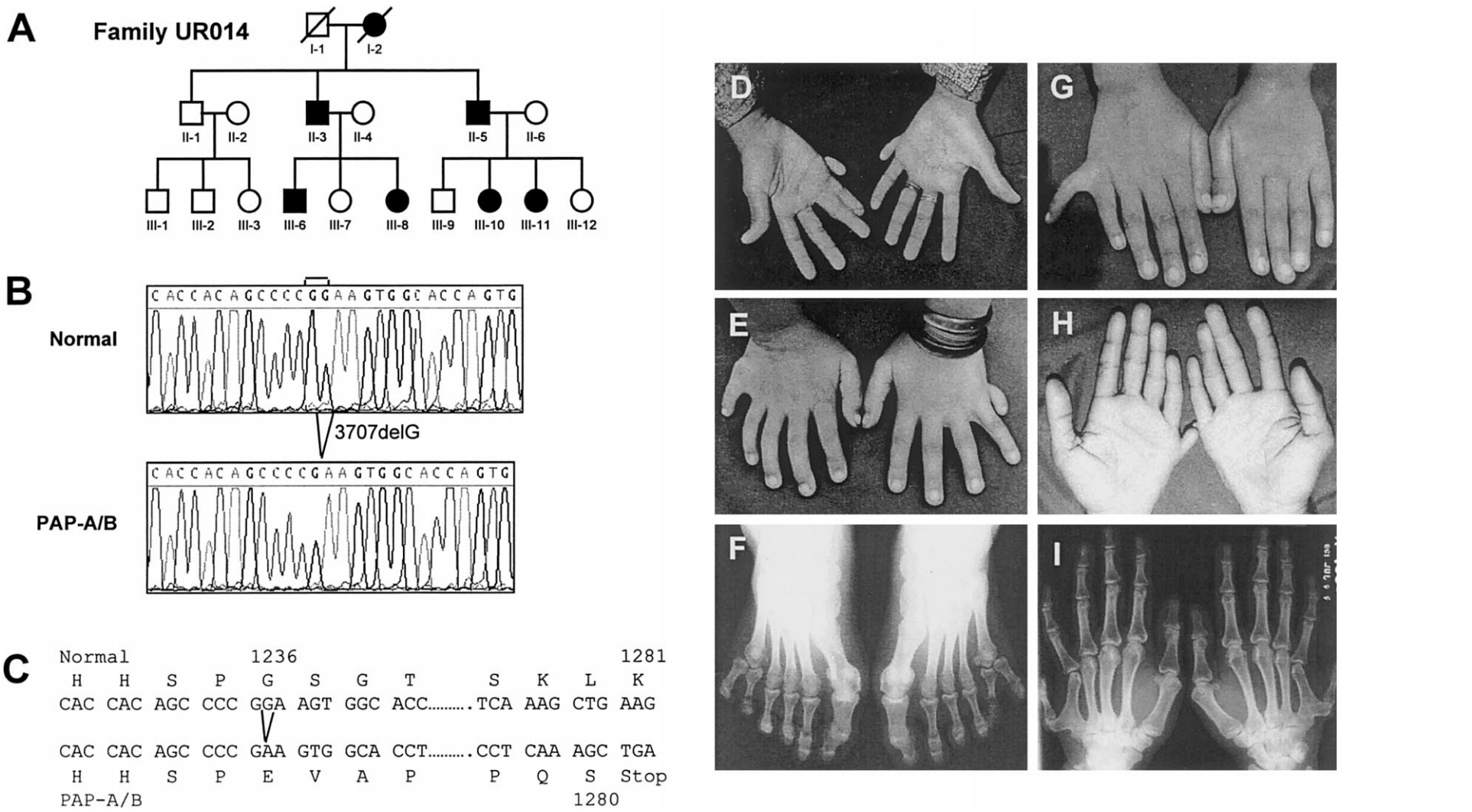

Figure 3 *A*, Partial pedigree of family UR014 with PAP-A/B. Affected individuals are shown with blackened symbols. *B*, Partial sequence of normal and PAP-A/B mutant from family UR014 showing deletion of G at nucleotide 3707. *C*, Comparison of normal and derived amino acid sequences due to the frameshift deletion mutation. The truncated protein is of 1281 amino acids after addition of 45 novel codons. *D–I*, Selected clinical and x-ray photographs from family UR014.

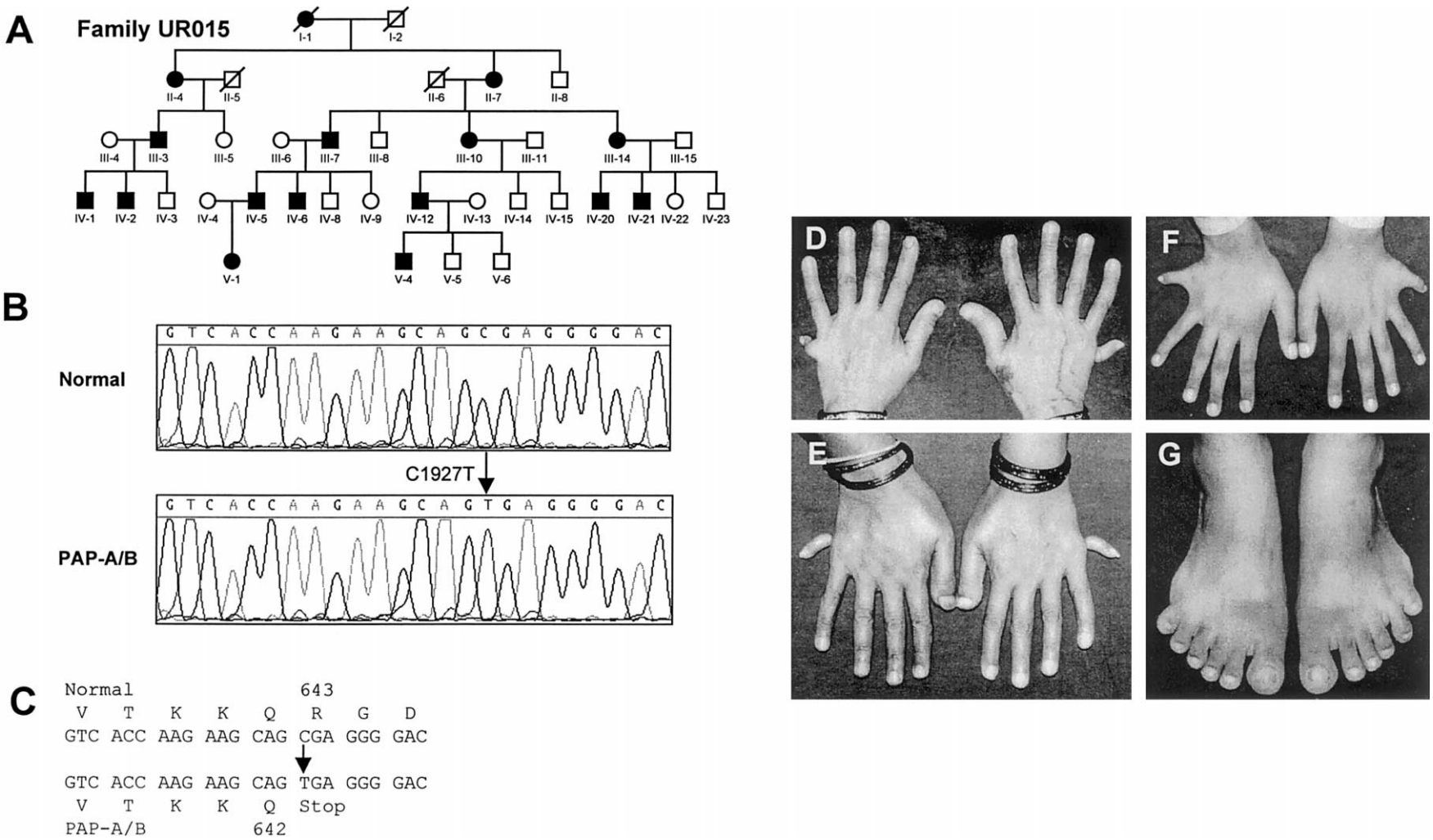

Figure 4 *A*, Partial pedigree from family UR015 with PAP-A/B phenotype. *B*, Partial nucleotide sequence from family UR015 showing the substitution of 1927C→T in GLI3, resulting in a stop codon (R643X). *C*, Comparison of translation products of the normal and mutated GLI3 allele. The truncated protein terminates at codon 643. *D–G*, Selected clinical photographs of different members of family UR015.

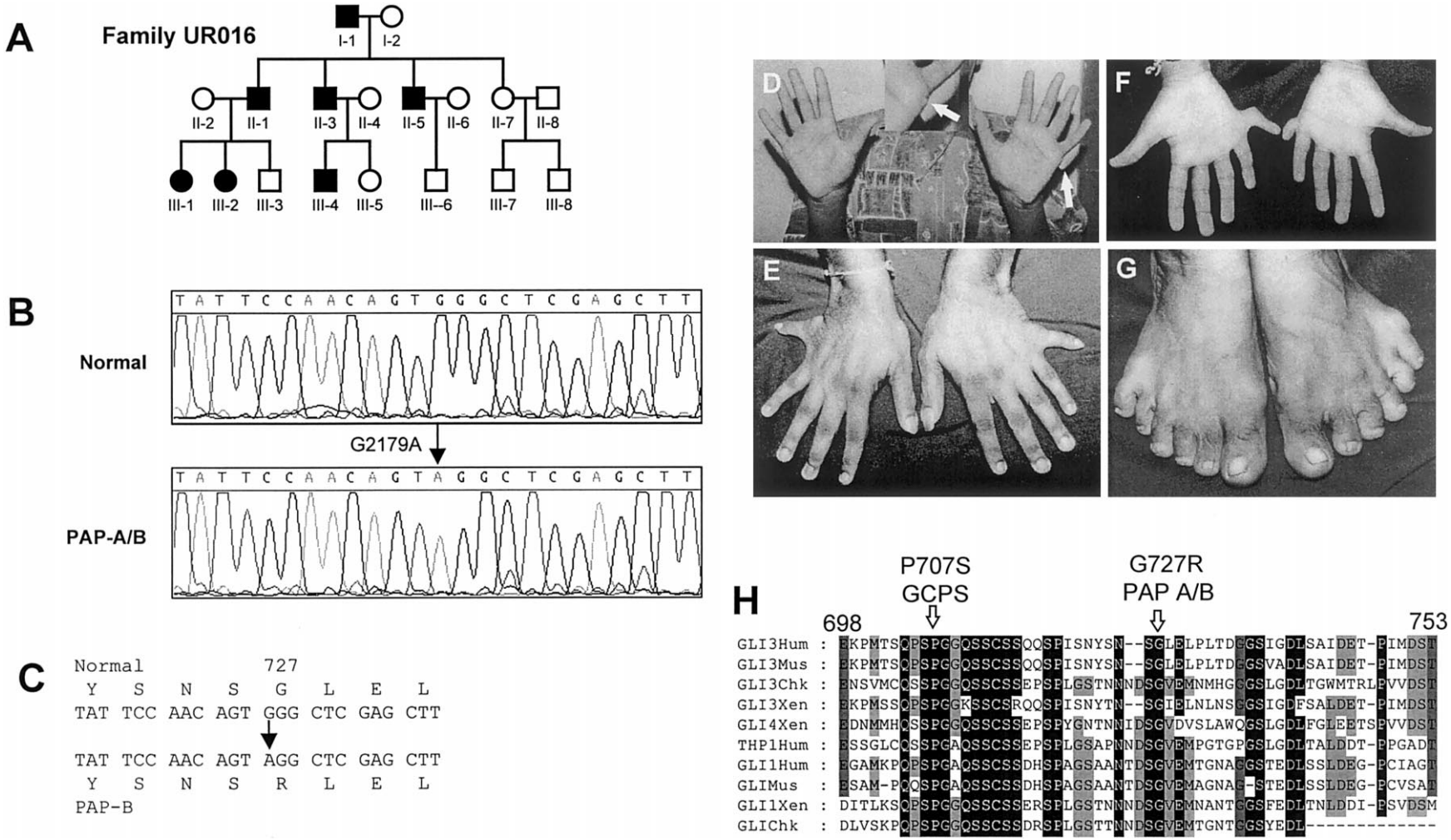

Figure 5 *A*, Partial pedigree of family UR016 with PAP-A/B phenotype. *B*, Comparison of normal and mutant nucleotide sequence in family UR016 shows a missence mutation resulting in a G→A transition 2179G→A, and the amino acid substitution G727R. *C*, Comparison of normal and derived amino acid sequences due to the missense mutation G727R. *D–G*, Selected clinical photographs of three affected individuals of family UR016. In panel *D*, the area of the pedunculated postminimus in the left hand of this individual is enlarged. *H*, Amino acid sequence comparisons of domain 3 from several members of the GLI family of proteins from different species. The conserved amino acid G727 mutated in family UR016, and the conserved P707 mutated in a reference patient with GCPS (Wild et al. 1997) are shown.

individuals in these pedigrees had any recognizable cranial or dental anomaly.

After we received informed consent, we collected blood samples from 66 affected and 22 normal individuals from these four pedigrees. Clinical information and photographs were collected from all affected individuals included in the study. Hand and foot x-rays were taken from selected individuals.

Family GVA02

The DNA of a patient with PHS ("patient-2") from family GVA02, who had been referred to the Medical Genetics Clinic of the University Hospital of Geneva, was also examined. A detailed description of the PHS phenotype of this patient and the family history were reported (Verloes et al. 1995).

Polymorphisms and Linkage Analysis

Genomic DNA was purified from peripheral blood lymphocytes according to standard SDS-proteinase-K and phenol/chloroform extraction method. DNA polymorphisms were analyzed by PCR amplification of short-sequence repeats. Polymorphic markers from chromosome 7p (D7S2848, D7S526, D7S795, D7S528, D7S521, D7S691, D7S667, and D7S478) were selected from the Généthon and the Cooperative Human Linkage Center collection (Murray et al. 1994; Dib et al. 1996) and were used as described (Radhakrishna et al. 1997*a*); in addition, two microsatellite polymorphisms—B48 and B81—within the GLI3 gene were also used (Kang et al. 1997*b*). One oligonucleotide primer of each marker was labeled with γ^{32}P-ATP by means of T4 polynucleotide kinase. PCR amplifications and scoring of the genotypes were performed as described (Blouin et al. 1995).

Linkage analysis was performed for markers within and around the GLI3 gene on chromosome 7p. Family information and marker genotypes were stored in pedigrees in the computer program Cyrillic (Cherwell). Two-point linkage analysis was performed by means of the MLINK and LINKMAP programs of LINKAGE v5.2 (Lathrop et al. 1984) and FASTLINK v3.0 (Cottingham et al. 1993) software packages. Maximum LOD and location scores were calculated for each marker locus by assuming autosomal dominant mode of inheritance with 100% penetrance. For all polymorphic markers, allele frequencies were kept equal.

Mutation Analysis

Genomic DNA from normal and affected individuals of the families described was PCR-amplified, using oligonucleotide primers, for 38 different genomic regions covering the entire coding sequence of GLI3 and all the splice junctions (Wild et al. 1997; Kang et al. 1997*a*). These PCR products were first screened for mutations by use of SSCP (Orita et al. 1989). The PCR products were denatured with an equal volume of 95% formamide, .05% xylene cyanol, and .05% bromophenol blue, for 15 minutes at 94°C, and loaded on a 12.5% GeneGel Excel (Pharmacia Biotech). Electrophoresis was at 600V at 12°C for 2–3 h, depending on the size of the PCR product. The gels were stained by DNA silver staining (Pharmacia Biotech). SSCP variants were purified and directly sequenced in both directions with appropriate primers by means of an ABI377 sequencer. Mutant alleles were also cloned by use of the Original TA cloning kit® (Invitrogen) after PCR amplification, purified as described elsewhere (Mehenni et al. 1998), and subjected to nucleotide sequencing.

Results

Mapping of Phenotypes to the Candidate 7p Region that Includes GLI3

Because mutations in the GLI3 gene were identified in families with PAP-A (Radhakrishna et al. 1997*b*), we first performed linkage analysis in the candidate genomic region of chromosome 7p in which the GLI3 gene is located, using DNA from families UR003, UR014, UR015, and UR016. A maximum LOD score was obtained with marker D7S521 ($Z_{max} = 8.12$; $\theta = .00$), which is located 0.42 cM centromeric to GLI3. No recombination was observed between this marker and the polydactyly phenotypes in all four families. The Z_{max} for families UR003, UR014, UR015, and UR016 were 3.91, 2.11, 1.11, and 0.99, respectively. We then used two microsatellite polymorphisms within the GLI3 gene (Kang et al. 1997*b*) in these families. No recombination with the GLI3 markers and the polydactyly phenotypes was observed in the informative members of these four families. The Z_{max} at $\theta = .00$ for the GLI3 markers were UR003: 5.51, UR014: 2.11, and UR015: 1.66. Family UR016 was not informative and yielded a $Z_{max} = 0.25$. These results suggested that the GLI3 gene was a strong candidate for the phenotypes in these four families and, subsequently, mutation analysis was performed.

Mutation Search in the GLI3 Gene

We then performed mutation analysis in all the coding regions and intron-exon junctions of the GLI3 gene in an affected and normal member of each family: UR003 with PPD-IV, UR014, UR015, UR016 with PAP-A/B, and GVA02 with PHS. The mutation search included SSCP and nucleotide sequencing of the abnormally migrating amplimers.

A single nucleotide insertion of C at GLI3 cDNA position 3647 in exon 15 (numbering as in GenBank accession numbers M57609–M34366) was found in heterozygosity in all affected members of family UR003

with PPD-IV. The insertion occurred in codon 1216 of the 1596–amino acid GLI3 in a (C)3 tract and results in a frameshift and stop codon at position 1245 after the addition of 30 novel amino acids at the carboxyl-terminus (fig. 2*B–C*).

In all affected members of family UR014 with PAP-A/B, a single nucleotide deletion of G in exon 15 was found in heterozygosity at position 3707 of GLI3 cDNA. This deletion occurred at codon 1236 in a (G)2 tract of one allele of GLI3, and this frameshift resulted in a stop codon at 1281 after the addition of 45 novel amino acids at the carboxyl-terminus (fig. 3*B–C*).

In the affected members of family UR015 with PAP-A/B, a C→T substitution was identified in heterozygosity in exon 13 at nucleotide position 1927 (1927C→T). This results in a nonsense codon CGA→TGA, which causes a premature stop at amino acid position 643 (R643X) (fig. 4*B, C*). The predicted truncation of the protein occurs between the zinc finger and domain 3 (or Pzf1) of GLI3.

Family UR016 showed a G→A substitution at nucleotide position 2179 of one GLI3 allele in all affected individuals. This results in the missense substitution Glycine→Arginine at codon 727 (G727R) (fig. 5*B, C*). This mutation occurred in domain 3 (or Pzf1), which is conserved in several species (fig. 5*H*). G727 is invariant in all domains 3 of the GLI family of proteins examined. No other mutation was identified in the entire coding region of this GLI3 allele. This exclusion was done not only by SSCP but by nucleotide sequencing of all amplicons from an affected individual of family UR016.

All the above mutations were present only in the affected individuals of these families and were absent in the unaffected members of these families. In addition, none of 100 unrelated normal individuals from the Gujarat region of India showed these mutations.

In patient GVA02, who reportedly had PHS (Verloes et al. 1995), a G→T substitution was identified in heterozygosity in exon 15 at nucleotide position 3439 (3439G→T). This results in a nonsense codon GAG→TAG that causes a premature stop at amino acid position 1147 (E1147X) (fig. 6*A, B*). The predicted truncation of the protein occurs after domain 5 of GLI3. This mutation was not present in the DNA of the parents and, therefore, had occurred de novo. In addition, this mutation was not found in the DNA of 100 normal Central European control subjects.

A single nucleotide variant G→T at position 4774 of the GLI3 cDNA, resulting in a nonsense codon GAA→TAA (E1592X), was found in some normal individuals from India. This polymorphism will result in a truncated GLI3 missing only five amino acids in the carboxyl-terminus (fig. 1).

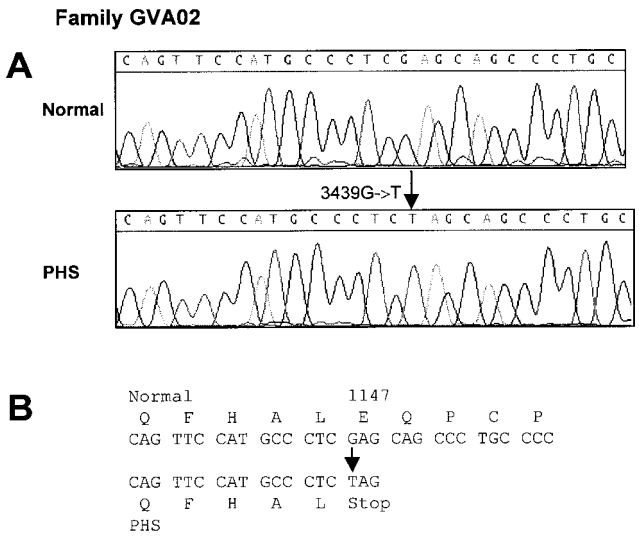

Figure 6 *A,* Partial sequence of normal and mutant GLI3 gene from the patient with PHS from family GVA02, showing the nucleotide substitution 3439G→T, which results in a stop codon (E147X). *B,* Comparison of normal and derived amino acid sequences due to the nonsense mutation E147X.

Discussion

The present mutation search adds two additional dominantly inherited phenotypes—PPD-IV and PAP-A/B—which are due to mutations in the GLI3 transcription regulator, thus extending the phenotypic spectrum (from 3 to 5) associated with GLI3 mutations.

That certain forms of the PAP-A/B phenotype are due to mutations in GLI3 is not entirely surprising, since some members of these families display only the PAP-A phenotype. It is of interest, however, that there are individuals with PAP-A in one hand and PAP-B in the other. This strongly suggests that the final phenotypic outcome may be due (in addition to the GLI3 mutations) to environmental or stochastic factors.

Remarkably, it has been suggested (Baraitser et al. 1983) that PPD-IV and GCPS may have the same molecular pathogenesis, since the digital changes of the two conditions are similar, although there are no craniofacial anomalies observed in PPD-IV. PPD-IV is characterized by PAP of the hand and PPD/PAP of the foot (Temtamy and McKusick 1978). In general, the deformities are more severe in the feet than in the hands. The thumb shows only the mildest degree of duplication, and syndactyly of various degrees affects fingers 3 and 4. Hand PAP is also occasionally present. The foot malformations are more penetrant and consist of duplication of part or all of the first toes and syndactyly of all the toes; PAP is also usually present (Reynolds et al. 1984). This dominant phenotype, also known as uncomplicated poly-

syndactyly type 1, or crossed polydactyly (CP1), due to the manifestation of polydactyly and syndactyly simultaneously, was defined as coexistence of PPD and PAP with discrepancy in the axis of polydactyly between the hands and the feet (Ishikiriyama et al. 1991).

The position of the GLI3 mutations found in this study does not conform to the hypothesis that defined truncations of the GLI3 protein are associated with specific phenotypes (Biesecker 1997; Radhakrishna et al. 1997*b*; Shin et al. 1999). More specifically: (1) The truncating nonsense mutation in codon 643 detected in family UR015 with PAP-A/B (fig. 1 and fig. 4*B, C*) is against the hypothesis that truncated GLI3 proteins that contain domain 3 are associated with PAP-A, whereas those with truncations upstream of domain 3 but containing the ZFD domain are associated with PHS. (2) The nonsense mutation found in the PHS patient would result in a truncated protein at codon 1147, which is in the C-terminal 3d of the protein well beyond the domain 5 (fig. 1 and fig. 6*A, B*). (3) The PPD-IV–associated mutation in family UR003 will truncate the protein at codon 1245 and that of PAP-A/B–associated mutation in family UR014 would result in a truncation at codon 1280 (fig. 1; fig. 2*B, C;* and fig. 3*B, C*). Although the novel amino acids at the C-termini of these aberrant proteins are different, the close position of these two mutations would predict a similar phenotype. (4) The amino acid substitution G727R in the UR016 family with PAP-A/B occurs in the well-conserved domain 3 (fig. 1 and fig. 5*B, C,* and *H*). Amino acid G727 is an invariant residue in all homologous proteins. If this mutation completely abolishes the function of GLI3, then the suggestion that haploinsufficiency of GLI3 is related to GCPS (Shin et al. 1999) may not be valid. Another amino acid substitution, P707S, at the invariant P707 residue of domain 3 has been found in a patient with GCPS (Wild et al. 1997). If these mutations result in a gain-of-function, then the expectation would be that these two patients would show similar phenotypes. We conclude from these phenotype-genotype observations that a simple correlation of the position of the GLI3 mutation and the resulting phenotype is far from satisfactory.

Several mouse phenotypes have been associated with mutations of GLi3 (see Jackson Laboratory database). These mutations, which affect the skeleton, eye, tail, and other appendages, are extra toes *Xt* (Johnson 1967; Hui and Joyner 1993); anterior digit deformity, recessive (*add*) (van der Hoeven et al. 1993); brachyphalangy, dominant (*bph*) (Johnson 1969); and polydactyly Nagoya, dominant (*pdn*) (Schimmang et al. 1994; Thien and Ruther 1999). These mutants display phenotypic variability of expression, and there is no apparent correlation between the site of mutation and the resulting phenotype. The *Xt* spontaneously induced mutation that occurred in a (C3Hx101)F2 mixed background shows variable expressivity and severity in affected homozygous and heterozygous mice. It is likely that the genetic background may contribute to the modification of the phenotype.

We propose that the syndromes associated with GLI3 mutations could be collectively called "GLI3 morphopathies." This term would cover, at present, five phenotypes—GCPS, PHS, PAP-A, PAP-A/B, and PPD-IV—and could be extended to other conditions yet unidentified. Since there is not an obvious phenotype-genotype correlation of GLI3 mutations and clinical outcome, and the "borders" of the phenotypic characterization among the different syndromes are not clear, we favor the designation of GLI3 morphopathies.

Acknowledgments

We thank U. C. Rao and T. R. Jani, for their assistance in collecting blood samples and ascertaining family members. We are grateful to all members of the UR003, UR014, UR015, UR016, and GVA02 families, for their cooperation and donation of blood samples. The study was supported by funds from the University and Cantonal Hospital of Geneva, and the Deutsche Forschungsgemeinschaft (373/20–2).

Electronic-Database Information

Accession numbers and URLs for data in this article are as follows:

The Cooperative Human Linkage Center: http://www.chlc.org/ (for polymorphic markers from chromosome 7p)
GenBank: http://www.ncbi.nlm.nih.gov/Web/Genbank/ (for cDNA position numbering)
Généthon: http://www.genethon.fr (for polymorphic markers from chromosome 7p)
Jackson Laboratory Informatics: http://www.informatics.jax.org/ (for mouse phenotypes associated with mutations of GLI3)
Online Mendelian Inheritance in Man (OMIM): http://www.ncbi.nlm.nih.gov/Omim/ (for PPD-IV [MIM 174700], GCPS [MIM 175700], PHS [MIM 146510], and PAP-A [MIM 147200]).

References

Aza-Blanc P, Ramirez-Weber FA, Laget MP, Schwartz C, Kornberg TB (1997) Proteolysis that is inhibited by hedgehog targets Cubitus interruptus protein to the nucleus and converts it to a repressor. Cell 89:1043–1053

Baraitser M, Winter RM, Brett EM (1983) Greig cephalopolysyndactyly: report of 13 affected individuals in three families. Clin Genet 24:257–265

Biesecker LG (1997) Strike three for GLI3. Nat Genet 17: 259–260

Blouin JL, Christie DH, Gos A, Lynn A, Morris MA, Ledbetter DH, Chakravarti A, et al (1995) A new dinucleotide repeat

polymorphism at the telomere of chromosome 21q reveals a significant difference between male and female rates of recombination. Am J Hum Genet 57:388–394

Cottingham RW Jr, Idury RM, Schaffer AA (1993) Faster sequential genetic linkage computations. Am J Hum Genet 53: 252–263

Dib C, Faure S, Fizames C, Samson D, Drouot N, Vignal A, Millasseau P, et al (1996) A comprehensive genetic map of the human genome based on 5,264 microsatellites. Nature 380:152–154

Dominguez M, Brunner M, Hafen E, Basler K (1996) Sending and receiving the hedgehog signal: control by the Drosophila Gli protein Cubitus interruptus. Science 272:1621–1625

Epstein CJ (1995) The new dysmorphology: application of insights from basic developmental biology to the understanding of human birth defects. Proc Natl Acad Sci USA 92:8566–8573

Hui CC, Joyner AL (1993) A mouse model of Greig cephalopolysyndactyly syndrome: the extra-toesJ mutation contains an intragenic deletion of the Gli3 gene. Nat Genet 3: 241–246

Ishikiriyama S, Sawada H, Nambu H, Niikawa N (1991) Crossed polydactyly type I in a mother and son: an autosomal dominant trait? Am J Med Genet 40:41–43

Johnson DR (1967) Extra-toes: a new mutant gene causing multiple abnormalities in the mouse. J Embryol Exp Morphol 17:543–581

——— (1969) Brachyphalangy, an allele of extra-toes in the mouse. Genet Res 13:275–280

Kang S, Graham JMJ, Olney AH, Biesecker LG (1997*a*) GLI3 frameshift mutations cause autosomal dominant Pallister-Hall syndrome. Nat Genet 15:266–268

Kang S, Rosenberg M, Ko VD, Biesecker LG (1997*b*) Gene structure and allelic expression assay of the human GLI3 gene. Hum Genet 101:154–157

Kucheria K, Kenue RK, Taneja N (1981) An Indian family with postaxial polydactyly in four generations. Clin Genet 20:36–39

Lathrop GM, Lalouel JM, Julier C, Ott J (1984) Strategies for multilocus linkage analysis in humans. Proc Natl Acad Sci USA 81:3443–3446

Mehenni H, Gehrig C, Nezu J, Oku A, Shimane M, Rossier C, Guex N, et al (1998) Loss of LKB1 kinase activity in Peutz-Jeghers syndrome, and evidence for allelic and locus heterogeneity. Am J Hum Genet 63:1641–1650

Murray JC, Buetow KH, Weber JL, Ludwigsen S, Scherpbier-Heddema T, Manion F, Quillen J, et al (1994) A comprehensive human linkage map with centimorgan density. Cooperative Human Linkage Center (CHLC). Science 265: 2049–2054

Orenic TV, Slusarski DC, Kroll KL, Holmgren RA (1990) Cloning and characterization of the segment polarity gene cubitus interruptus dominant of Drosophila. Genes Dev 4: 1053–1067

Orita M, Iwahana H, Kanazawa H, Hayashi K, Sekiya T (1989) Detection of polymorphisms of human DNA by gel electrophoresis as single-strand conformation polymorphisms. Proc Natl Acad Sci USA 86:2766–2770

Radhakrishna U, Blouin JL, Mehenni H, Patel UC, Patel MN, Solanki JV, Antonarakis SE (1997*a*) Mapping one form of autosomal dominant postaxial polydactyly type A to chromosome 7p15-q11.23 by linkage analysis. Am J Hum Genet 60:597–604

Radhakrishna U, Wild A, Grzeschik KH, Antonarakis SE (1997*b*) Mutation in GLI3 in postaxial polydactyly type A. Nat Genet 17:269–271

Reynolds JF, Sommer A, Kelly TE (1984) Preaxial polydactyly type 4: variability in a large kindred. Clin Genet 25:267–272

Robbins DJ, Nybakken KE, Kobayashi R, Sisson JC, Bishop JM, Therond PP (1997) Hedgehog elicits signal transduction by means of a large complex containing the kinesin-related protein costal2. Cell 90:225–234

Ruiz i Altaba A (1997) Catching a Gli-mpse of Hedgehog. Cell 90:193–196

Ruppert JM, Vogelstein B, Arheden K, Kinzler KW (1990) GLI3 encodes a 190-kilodalton protein with multiple regions of GLI similarity. Mol Cell Biol 10:5408–5415

Schimmang T, Oda SI, Ruther U (1994) The mouse mutant Polydactyly Nagoya (Pdn) defines a novel allele of the zinc finger gene Gli3. Mamm Genome 5:384–386

Shin SH, Kogerman P, Lindstrom E, Toftgard R, Biesecker LG (1999) GLI3 mutations in human disorders mimic Drosophila cubitus interruptus protein functions and localization. Proc Natl Acad Sci USA 96:2880–2884

Sisson JC, Ho KS, Suyama K, Scott MP (1997) Costal2, a novel kinesin-related protein in the hedgehog signaling pathway. Cell 90:235–245

Temtamy SA, McKusick VA (1969) Synopsis of hand malformation with particular emphasis on genetic factors. Birth Defects 5:125–184

——— (1978) The genetics of hand malformations. Alan R. Liss, New York

Thien H, Ruther U (1999) The mouse mutation Pdn (Polydactyly Nagoya) is caused by the integration of a retrotransposon into the Gli3 gene. Mamm Genome 10:205–209

van der Hoeven F, Schimmang T, Vortkamp A, Ruther U (1993) Molecular linkage of the morphogenetic mutation add and the zinc finger gene Gli3. Mamm Genome 4: 276–277

Verloes A, David A, Ngo L, Bottani A (1995) Stringent delineation of Pallister-Hall syndrome in two long surviving patients: importance of radiological anomalies of the hands. J Med Genet 32:605–611

Vortkamp A, Gessler M, Grzeschik KH (1991) GLI3 zinc-finger gene interrupted by translocations in Greig syndrome families. Nature 352:539–540

Wild A, Kalff-Suske M, Vortkamp A, Bornholdt D, Konig R, Grzeschik KH (1997) Point mutations in human GLI3 cause Greig syndrome. Hum Mol Genet 6:1979–1984